

Self-propelled Brownian spinning top: Dynamics of a biaxial swimmer at low Reynolds numbers

Raphael Wittkowski and Hartmut Löwen

Institut für Theoretische Physik II, Weiche Materie, Heinrich-Heine-Universität Düsseldorf, D-40225 Düsseldorf, Germany

(Received 26 September 2011; revised manuscript received 30 December 2011; published 21 February 2012)

Recently the Brownian dynamics of self-propelled (active) rodlike particles was explored to model the motion of colloidal microswimmers, catalytically driven nanorods, and bacteria. Here we generalize this description to biaxial particles with arbitrary shape and derive the corresponding Langevin equation for a self-propelled Brownian spinning top. The biaxial swimmer is exposed to a hydrodynamic Stokes friction force at low Reynolds numbers, to fluctuating random forces and torques as well as to an external and an internal (effective) force and torque. The latter quantities control its self-propulsion. Due to biaxiality and hydrodynamic translational-rotational coupling, the Langevin equation can only be solved numerically. In the special case of an orthotropic particle in the absence of external forces and torques, the noise-free (zero-temperature) trajectory is analytically found to be a circular helix. This trajectory is confirmed numerically to be more complex in the general case of an arbitrarily shaped particle under the influence of arbitrary forces and torques involving a transient irregular motion before ending up in a simple periodic motion. By contrast, if the external force vanishes, no transient regime is found, and the particle moves on a *superhelical* trajectory. For orthotropic particles, the noise-averaged trajectory is a generalized *concho-spiral*. We furthermore study the reduction of the model to two spatial dimensions and classify the noise-free trajectories completely finding circles, straight lines with and without transients, as well as cycloids and arbitrary periodic trajectories.

DOI: [10.1103/PhysRevE.85.021406](https://doi.org/10.1103/PhysRevE.85.021406)

PACS number(s): 82.70.Dd, 05.40.Jc

I. INTRODUCTION

In the traditional description of colloidal particles, their shape is assumed to be either spherical or rodlike [1–3], or, in other words, the particles are either isotropic or uniaxial, i.e., rotationally symmetric around a figure axis [4–8]. In the isotropic case, the location of the particle is described by its center-of-mass position, while for uniaxial particles an additional unit vector is needed to describe its orientation. Using various preparation techniques, by now, it is possible to prepare colloidal particles with a more complex shape than spherical and uniaxial in a controlled way [9–14]. In particular, it is possible to synthesize particles with an orthotropic shape such as, for example, board-like colloids [15]. However, while the theory of Brownian dynamics for spherical and uniaxial colloidal particles is quite advanced [1,2,16,17], much less is known for biaxial particles, which need an additional angle to describe their location in space (on top of the center-of-mass position and the orientational unit vector). This additional degree of freedom complicates the description of Brownian motion considerably [18,19].

A second recent development in colloid science is to make the colloidal particles self-propelling such that they are moving in space on their own (so-called *active* particles) [20,21]. There are numerous examples of self-propelling colloidal particles including catalytically driven nanorods [22–25] and thermogradient-driven Janus particles [26], not to speak of other realizations of swimmers in vibrating granulates [27], magnetic beads [28], and real biological systems [29–37], where, for example, protozoa use cilia, flagella, traveling waves, and protoplasmic flow for locomotion [38]. The simplest description of self-propulsion is modeled by an internal effective force, which provides an constant propulsion mechanism on top of the Brownian motion of the particle.¹

In two spatial dimensions, it was shown recently that the simultaneous action of an internal force and an internal torque leads to circle swimming [27,39], and in three spatial dimensions, the behavior of the mean square displacement was calculated analytically [40–42].

All considerations for Brownian swimmers were done hitherto for uniaxial particles. We are not aware of any study for biaxial swimmers except for a recent modeling by Vogel and Stark [43]. This is important for at least two reasons: First, real particles are in general not uniaxial, and therefore the effect of biaxiality needs to be studied. Second, it is of general importance to generalize the equations of a “Brownian spinning top” toward self-propulsion in order to understand and predict its motion on a fundamental level. Surprisingly, while the spinning top in an external field governed by the Newtonian (or Eulerian) equations is a standard reference model in classical mechanics, there are only few studies for overdamped Brownian motion of a passive spinning top [44,45].

In this paper we derive the Langevin equation for a biaxial self-propelled particle with arbitrary shape that may even be screw-like, implying a translational-rotational coupling [46,47]. The biaxial swimmer is exposed to a hydrodynamic Stokes friction force at low Reynolds numbers, to fluctuating random forces and torques, as well as to an external and an internal (effective) force and torque. The internal force and torque control the translational and angular propulsion velocity and are constant in the body-fixed frame while the external force and torque are constant in the space-fixed laboratory frame.

Due to biaxiality and hydrodynamic translational-rotational coupling, the Langevin equation can only be solved numerically. In the special case of an orthotropic particle, which has no translational-rotational coupling, the noise-free (zero-temperature) trajectory is analytically found to be a circular helix in the absence of any external force and torque. Such helix-like trajectories are indeed typical

¹This should not be confused with the basic fact that a swimmer is force free and torque free.

for swimming microorganisms [38,48]. The trajectories are confirmed numerically to be much more complex in the general case. Typically there is an irregular transient motion before the particle ends up in a simple periodic motion. By contrast, if the external force vanishes, no transient motion shows up and the particle exhibits a *superhelical* trajectory. For orthotropic particles, the noise-averaged trajectory is studied numerically and found to be a generalized *concho-spiral* [49] with a “snail-shell” structure. We furthermore study the reduction of the model to two spatial dimensions, where there is only one orientational angle and the internal and external torques can be combined to a single effective torque. In this simpler two-dimensional limit, we classify the noise-free trajectories completely. Circles are found in the absence of the external force. In general, the trajectories are straight lines with and without transients as well as cycloids and arbitrary periodic curves.

This paper is organized as follows: In Sec. II we present the Langevin equation for a general self-propelled rigid biaxial Brownian particle in an unbounded viscous fluid with low Reynolds number being at rest at infinity. Section III is dedicated to special analytical solutions and Sec. IV to more general numerical calculations for the Langevin equation. Finally, we conclude and give an outlook in Sec. V.

II. LANGEVIN EQUATION

In this section we describe the Brownian motion of a biaxial self-propelled particle suspended in an unbounded viscous fluid at rest at infinity for low Reynolds numbers. It is assumed that the colloidal particle is rigid and has a constant mass density. The motion of such a particle is characterized by the translational center-of-mass velocity $\dot{\vec{r}} = d\vec{r}/dt$ with the center-of-mass position $\vec{r}(t)$ and the time variable t as well as by the instantaneous angular velocity $\vec{\omega}(t)$. The Brownian motion of colloidal particles with arbitrary shape involves a hydrodynamic coupling between the translational and the rotational degrees of freedom, which was described theoretically, for example, by Brenner [46,47]. In 2002 Fernandes and de la Torre [44] proposed a corresponding Brownian dynamics simulation algorithm for the motion of a passive rigid particle with arbitrary shape. The underlying equations of motion were generalized toward an imposed external flow field for the surrounding fluid by Makino and Doi [45].

Here we appropriately generalize this description to *internal* degrees of freedom, i.e., to a self-propelled biaxial particle, which experiences an internal effective force \vec{F}_0 and torque T_0 , which are both constant in a body-fixed coordinate system. This models a biaxial microswimmer. Of course, a swimmer is in principle force free and torque free, but the internal force and torque are meant to be effective quantities, which govern the propulsion mechanism of the particle. Using a compact notation, we introduce the basic completely overdamped *Langevin equation for three spatial dimensions*

$$\vec{v} = \beta \mathcal{D}(\vec{r}) [\mathcal{R}^{-1}(\vec{r}) \vec{K}_0 - \vec{\nabla}_{\vec{r}} U(\vec{r}) + \mathcal{R}^{-1}(\vec{r}) \vec{k}] + \vec{\nabla}_{\vec{r}} \cdot \mathcal{D}(\vec{r}) \quad (1)$$

for a self-propelled Brownian spinning top (see the Appendix for a derivation). At first, we explain the notation step by

step. The biaxial particle has the position $\vec{r}(t) = (x_1, x_2, x_3)$ and the orientation $\vec{\omega}(t) = (\phi, \theta, \chi)$, which is given in Eulerian angles.² We summarize translational and rotational degrees of freedom by a compact six-dimensional vector $\vec{x} = (\vec{r}, \vec{\omega})$, which obviously involves a generalized velocity $\vec{v} = (\dot{\vec{r}}, \dot{\vec{\omega}})$ (with $\dot{\vec{\omega}}$ denoting the angular velocity) and a gradient $\vec{\nabla}_{\vec{x}} = (\vec{\nabla}_{\vec{r}}, \vec{\nabla}_{\vec{\omega}})$. This gradient operator is composed of the usual translational gradient operator $\vec{\nabla}_{\vec{r}} = (\partial_{x_1}, \partial_{x_2}, \partial_{x_3})$ acting on the Cartesian coordinates of \vec{r} and of the rotational gradient operator $\vec{\nabla}_{\vec{\omega}} = i\hat{L}$ [50] given by the product of the imaginary unit i and the angular momentum operator $\hat{L} = (L_1, L_2, L_3)$ in Eulerian angles. In the space-fixed coordinate system, the angular momentum operator \hat{L} is given in Eulerian angles by [50]

$$iL_1 = -\cos(\phi) \cot(\theta) \partial_\phi - \sin(\phi) \partial_\theta + \cos(\phi) \csc(\theta) \partial_\chi, \quad (2)$$

$$iL_2 = -\sin(\phi) \cot(\theta) \partial_\phi + \cos(\phi) \partial_\theta + \sin(\phi) \csc(\theta) \partial_\chi, \quad (3)$$

$$iL_3 = \partial_\phi. \quad (4)$$

The angular velocity $\vec{\omega}$ is expressed in Eulerian angles by

$$\vec{\omega} = M(\vec{\omega}) \dot{\vec{\omega}} \quad (5)$$

with the tensor [51]

$$M(\vec{\omega}) = \begin{pmatrix} 0 & -\sin(\phi) & \cos(\phi) \sin(\theta) \\ 0 & \cos(\phi) & \sin(\phi) \sin(\theta) \\ 1 & 0 & \cos(\theta) \end{pmatrix}, \quad (6)$$

$$M^{-1}(\vec{\omega}) = \begin{pmatrix} -\cos(\phi) \cot(\theta) & -\sin(\phi) \cot(\theta) & 1 \\ -\sin(\phi) & \cos(\phi) & 0 \\ \cos(\phi) \csc(\theta) & \sin(\phi) \csc(\theta) & 0 \end{pmatrix}, \quad (7)$$

and the time derivatives $\dot{\vec{\omega}} = d\vec{\omega}/dt$ of the Eulerian angles $\vec{\omega}(t)$. Furthermore, in Eq. (1) the compact notation $\vec{K}_0 = (\vec{F}_0, T_0)$ for the generalized force is used, which combines the effective propulsion force and torque. In general, the biaxial particle is also exposed to an external potential $U(\vec{r})$ giving rise to an external force $\vec{F}_{\text{ext}} = -\vec{\nabla}_{\vec{r}} U$ and an external torque $T_{\text{ext}} = -\vec{\nabla}_{\vec{\omega}} U$, which we consider to be constant in the sequel in order to keep the model simple.

The 6×6 -dimensional matrix $\mathcal{R}^{-1}(\vec{r})$ in Eq. (1) is associated with the geometric transformation from the body-fixed frame to the space-fixed laboratory frame. Its inverse $\mathcal{R}(\vec{r})$ is the block diagonal rotation matrix

$$\mathcal{R}(\vec{r}) = \text{diag}(\mathbf{R}(\vec{\omega}), \mathbf{R}(\vec{\omega})) \quad (8)$$

²As there is no uniqueness in the definitions of the Eulerian angles $\vec{\omega} = (\phi, \theta, \chi)$, we use for convenience the popular convention of Gray and Gubbins [50], which is equivalent to the second convention of Schutte [51]. This convention has the advantage that it is a direct generalization of the spherical coordinates (θ, ϕ) that are identical with the first two Eulerian angles ϕ and θ , while the third angle χ describes the rotation around the axis that is defined by θ and ϕ in the spherical coordinate system.

with the submatrices

$$\begin{aligned} \mathbf{R}(\vec{\omega}) &= \mathbf{R}_3(\chi) \mathbf{R}_2(\theta) \mathbf{R}_3(\phi), \\ \mathbf{R}^{-1}(\vec{\omega}) &= \mathbf{R}^T(\vec{\omega}) = \mathbf{R}_3(-\phi) \mathbf{R}_2(-\theta) \mathbf{R}_3(-\chi), \end{aligned} \quad (9)$$

where the elementary rotation matrices $\mathbf{R}_i(\varphi)$ describe a clockwise rotation (when looking down the axes) around the i th Cartesian axis by the angle φ for $i \in \{1, 2, 3\}$:

$$\mathbf{R}_1(\varphi) = \begin{pmatrix} 1 & 0 & 0 \\ 0 & \cos(\varphi) & \sin(\varphi) \\ 0 & -\sin(\varphi) & \cos(\varphi) \end{pmatrix}, \quad (10)$$

$$\mathbf{R}_2(\varphi) = \begin{pmatrix} \cos(\varphi) & 0 & -\sin(\varphi) \\ 0 & 1 & 0 \\ \sin(\varphi) & 0 & \cos(\varphi) \end{pmatrix}, \quad (11)$$

$$\mathbf{R}_3(\varphi) = \begin{pmatrix} \cos(\varphi) & \sin(\varphi) & 0 \\ -\sin(\varphi) & \cos(\varphi) & 0 \\ 0 & 0 & 1 \end{pmatrix}. \quad (12)$$

The particle shape and its hydrodynamic properties enter the Langevin equation in the generalized short-time diffusion (or inverse friction) tensor $\mathcal{D}(\vec{\mathfrak{r}})$. This can be expressed as the 6×6 -dimensional matrix

$$\begin{aligned} \mathcal{D}(\vec{\mathfrak{r}}) &= \begin{pmatrix} \mathbf{D}^{\text{TT}}(\vec{\omega}) & \mathbf{D}^{\text{TR}}(\vec{\omega}) \\ \mathbf{D}^{\text{RT}}(\vec{\omega}) & \mathbf{D}^{\text{RR}}(\vec{\omega}) \end{pmatrix} \\ &= \frac{1}{\beta\eta} \mathcal{R}^{-1}(\vec{\mathfrak{r}}) \mathcal{H}^{-1} \mathcal{R}(\vec{\mathfrak{r}}), \end{aligned} \quad (13)$$

where $\mathbf{D}^{\text{TT}}(\vec{\omega})$, $\mathbf{D}^{\text{TR}}(\vec{\omega}) = (\mathbf{D}^{\text{RT}}(\vec{\omega}))^T$, and $\mathbf{D}^{\text{RR}}(\vec{\omega})$ are 3×3 -dimensional submatrices, which correspond to pure translation, translational-rotational coupling, and pure rotation, respectively.³ Here η is the dynamic (shear) viscosity of the embedding fluid and $\beta = 1/(k_B T)$ with the Boltzmann constant k_B and the absolute (effective) temperature T denotes the inverse thermal energy. The matrix \mathcal{H} is constant and depends only on the shape and the size of the Brownian particle. It is composed of the symmetric translation tensor \mathbf{K} , the not necessarily symmetric coupling tensor \mathbf{C}_S ,⁴ and the symmetric rotation tensor Ω_S [47,52]:

$$\mathcal{H} = \begin{pmatrix} \mathbf{K} & \mathbf{C}_S^T \\ \mathbf{C}_S & \Omega_S \end{pmatrix}. \quad (14)$$

The matrix \mathcal{H} thus involves altogether 21 shape-dependent parameters. If the considered particle has a symmetric shape, many elements of the matrix \mathcal{H} are zero and the total number of shape-dependent parameters is much smaller. Especially for particle shapes without a hydrodynamic translational-rotational coupling, the coupling tensor \mathbf{C}_S vanishes and at most 12 shape-dependent parameters remain, if the coordinate system is chosen appropriately. An example for such particles without a hydrodynamic translational-rotational coupling is orthotropic particles. For these particles, the matrix \mathcal{H} is

even diagonal, implying only six shape-dependent parameters. Rodlike particles with rotational symmetry about a figure axis and additional head-tail symmetry are still more symmetric. Two of the first three as well as the last three diagonal elements of the matrix \mathcal{H} are equal for rodlike particles so that there are only three shape-dependent parameters left. The most symmetric shape is the sphere. For spherical particles, there are only two shape-dependent parameters. The first one is related to translation and appears in the first three diagonal elements of \mathcal{H} , while the second parameter is associated with rotation and appears in the last three diagonal elements of the matrix \mathcal{H} . The general connection of the symmetry properties of the particle shape with the structure of the matrix \mathcal{H} is described in detail in Ref. [52].

Finally, $\vec{k}(t) = (\vec{f}_0, \vec{\tau}_0)$ denotes the stochastic force $\vec{f}_0(t)$ and torque $\vec{\tau}_0(t)$ due to thermal fluctuations, which act on the Brownian particle in body-fixed coordinates for $T > 0$. This thermal noise $\vec{k}(t)$ is assumed to be Gaussian white noise with mean

$$\langle \vec{k}(t) \rangle = \vec{0} \quad (15)$$

and correlation

$$\langle \vec{k}(t_1) \otimes \vec{k}(t_2) \rangle = \mathcal{H} \frac{2\eta}{\beta} \delta(t_1 - t_2), \quad (16)$$

where $\langle \cdot \rangle$ denotes the noise average.

We remark that the dynamics, which is described by the Langevin equation, depends on the definition of the stochastic contribution $\propto \vec{k}(t)$. In the present form, the Langevin equation is only valid if the multiplicative noise is defined in the Itô sense [53]. Then the additive drift term $\vec{\nabla}_{\vec{\mathfrak{r}}} \cdot \mathcal{D}(\vec{\mathfrak{r}})$ at the end of the Langevin equation guarantees that the solutions of the Langevin equation respect the Boltzmann distribution, when the system is in thermodynamic equilibrium at temperature T . Other definitions than that of Itô, for example, the Stratonovich formulation, require a modification of the drift term [54]. This circumstance is always relevant in the case of multiplicative noise, but the necessity of the adaptation of the Langevin equation to the definition of the stochastic noise has been missed in previous work [44,45].

III. SPECIAL ANALYTICAL SOLUTIONS OF THE LANGEVIN EQUATION

The Langevin equation (1) represents a system of six coupled nonlinear stochastic differential equations [55] that cannot be solved analytically in general. There exist only a few analytical solutions for rather special situations. Several simple Langevin equations for self-propelled spherical or uniaxial particles in two or three spatial dimensions are known from the literature [39–41] and appear to be special cases of our general Langevin equation (1). These Langevin equations are not as general and complicated as Eq. (1) and can be solved analytically. Other analytically solvable special cases of Eq. (1) are obtained for orthotropic particles in the absence of thermal fluctuations.

A. Three spatial dimensions

In the general three-dimensional case, it is not even possible to solve the Langevin equation (1) analytically, if the stochastic

³For experimental investigations of the three-dimensional translational and rotational diffusion of biaxial colloidal particles, see, for example, Refs. [70,71] and references therein.

⁴The coupling tensor becomes symmetric if one chooses the *center of hydrodynamic reaction* as reference point S [52].

noise is neglected. Further simplifications that reduce the number of the degrees of freedom or diagonalize the matrix \mathcal{H} are necessary in order to obtain soluble cases.

B. Two spatial dimensions

An obvious simplification of the general Langevin equation (1) is the restriction to two spatial dimensions. A two-dimensional analog of the general Langevin equation can be obtained by choosing $x_3 = 0$, $\theta = \pi/2$, and $\chi = 0$ leaving only a single azimuthal angle ϕ . In analogy to the notation in Ref. [39], we further define $\mathcal{R}^{-1}(\vec{x})\vec{K}_0 = (\vec{F}_A, 0, 0, 0, M)$, $\vec{k}(t) = (0, f_\perp, f_\parallel, -\tau, 0, 0)$, and $\mathcal{R}^{-1}(\vec{x})\vec{k} = (\vec{f}, 0, 0, 0, \tau)$, where $\vec{F}_A = F_\parallel \hat{u}_\parallel + F_\perp \hat{u}_\perp$ is the internal driving force and M is the internal driving torque. The orientation vector $\hat{u}_\parallel = (\cos(\phi), \sin(\phi))$ denotes the figure axis of the particle, and $\hat{u}_\perp = (-\sin(\phi), \cos(\phi))$ is its orthogonal complement. Similarly, the vector $\vec{f}(t)$ denotes the stochastic force, and $\tau(t)$ is the stochastic torque acting on the particle. The stochastic force vector $\vec{f}(t)$ is decomposed like the internal driving force: $\vec{f}(t) = f_\parallel \hat{u}_\parallel + f_\perp \hat{u}_\perp$. Moreover, the new two-dimensional position vector is $\vec{r} = (x_1, x_2)$, the corresponding gradient is $\vec{\nabla}_{\vec{r}} = (\partial_{x_1}, \partial_{x_2})$, and the stochastic noise is characterized by the vector $\vec{\xi}(t) = (f_\perp, f_\parallel, -\tau)$ with mean

$$\langle \vec{\xi}(t) \rangle = \vec{0} \quad (17)$$

and correlation

$$\langle \vec{\xi}(t_1) \otimes \vec{\xi}(t_2) \rangle = \tilde{\mathcal{H}} \frac{2\eta}{\beta} \delta(t_1 - t_2), \quad (18)$$

where $\tilde{\mathcal{H}} = (\mathcal{H}_{ij})_{i,j=2,3,4}$ is a 3×3 -dimensional submatrix of \mathcal{H} . The Langevin equations for two spatial dimensions are then given by

$$\begin{aligned} \dot{\vec{r}} &= \vec{B}_1 + \beta[\mathcal{D}_T(\vec{F}_A - \vec{\nabla}_{\vec{r}}U + \vec{f}) - \vec{D}_C(M - \partial_\phi U + \tau)], \\ \dot{\phi} &= \beta[\mathcal{D}_R(M - \partial_\phi U + \tau) - \vec{D}_C \cdot (\vec{F}_A - \vec{\nabla}_{\vec{r}}U + \vec{f})] \end{aligned} \quad (19)$$

with the drift vector

$$\vec{B}_1(\phi) = B_1^\parallel \hat{u}_\parallel + B_1^\perp \hat{u}_\perp, \quad (20)$$

which is in accordance with the interpretation of the solution of the Langevin equations as an Itô process [56], the translational short-time diffusion tensor

$$\begin{aligned} \mathcal{D}_T(\phi) &= D_1 \hat{u}_\parallel \otimes \hat{u}_\parallel + D_2 (\hat{u}_\parallel \otimes \hat{u}_\perp + \hat{u}_\perp \otimes \hat{u}_\parallel) \\ &\quad + D_3 \hat{u}_\perp \otimes \hat{u}_\perp, \end{aligned} \quad (21)$$

TABLE I. Connection between the symmetry of the particle shape and the parameters (23)–(30) in the Langevin equations (19) for two spatial dimensions.

Type of shape	Symmetries	Invariance properties	Shape-dependent parameters	
			$D_1 \neq 0, D_R \neq 0$	
Uniaxial	No symmetry	–	$B_1^\parallel \neq 0, B_1^\perp \neq 0, D_2 \neq 0, D_3 \neq 0, D_C^\parallel \neq 0, D_C^\perp \neq 0$	
Uniaxial	Inflection symmetry	$x_1 \rightarrow -x_1$	$B_1^\parallel = 0, B_1^\perp \neq 0, D_2 = 0, D_3 \neq 0, D_C^\parallel \neq 0, D_C^\perp = 0$	
		$x_2 \rightarrow -x_2$	$B_1^\parallel \neq 0, B_1^\perp = 0, D_2 = 0, D_3 \neq 0, D_C^\parallel = 0, D_C^\perp \neq 0$	
Uniaxial	Inflection symmetry	$x_1 \rightarrow -x_1, x_2 \rightarrow -x_2$	$B_1^\parallel = 0, B_1^\perp = 0, D_2 = 0, D_3 \neq 0, D_C^\parallel = 0, D_C^\perp = 0$	
Isotropic	Rotational symmetry	$\phi \rightarrow \phi + \Delta\phi \forall \Delta\phi \in [0, 2\pi)$	$B_1^\parallel = 0, B_1^\perp = 0, D_2 = 0, D_3 = D_1, D_C^\parallel = 0, D_C^\perp = 0$	

and the coupling vector

$$\vec{D}_C(\phi) = D_C^\parallel \hat{u}_\parallel + D_C^\perp \hat{u}_\perp. \quad (22)$$

They involve only 8 instead of 21 shape-dependent parameters. These are the translational drift coefficients

$$B_1^\parallel = \frac{1}{\beta\eta} [(\mathcal{H}^{-1})_{24} - (\mathcal{H}^{-1})_{15}], \quad (23)$$

$$B_1^\perp = \frac{1}{\beta\eta} [(\mathcal{H}^{-1})_{16} - (\mathcal{H}^{-1})_{34}], \quad (24)$$

the translational diffusion coefficients

$$D_1 = \frac{1}{\beta\eta} (\mathcal{H}^{-1})_{33} = \frac{1}{\beta\eta} (\tilde{\mathcal{H}}^{-1})_{22}, \quad (25)$$

$$D_2 = \frac{1}{\beta\eta} (\mathcal{H}^{-1})_{23} = \frac{1}{\beta\eta} (\tilde{\mathcal{H}}^{-1})_{12}, \quad (26)$$

$$D_3 = \frac{1}{\beta\eta} (\mathcal{H}^{-1})_{22} = \frac{1}{\beta\eta} (\tilde{\mathcal{H}}^{-1})_{11}, \quad (27)$$

the coupling coefficients

$$D_C^\parallel = \frac{1}{\beta\eta} (\mathcal{H}^{-1})_{34} = \frac{1}{\beta\eta} (\tilde{\mathcal{H}}^{-1})_{23}, \quad (28)$$

$$D_C^\perp = \frac{1}{\beta\eta} (\mathcal{H}^{-1})_{24} = \frac{1}{\beta\eta} (\tilde{\mathcal{H}}^{-1})_{13}, \quad (29)$$

and the rotational diffusion coefficient

$$D_R = \frac{1}{\beta\eta} (\mathcal{H}^{-1})_{44} = \frac{1}{\beta\eta} (\tilde{\mathcal{H}}^{-1})_{33}. \quad (30)$$

Similar to the case of three spatial dimensions, some of these eight coefficients are zero or equal, respectively, if the described Brownian particle is symmetric. Table I gives an overview of possible symmetries of the particle's shape and the corresponding properties of the shape-dependent coefficients (23)–(30).

Although the Langevin equations (19) for two spatial dimensions are much simpler than Eq. (1), they are still coupled nonlinear stochastic differential equations and thus not analytically solvable. However, if the external potential $U(\vec{r}, \phi)$ is set to zero, the Langevin equations can be solved analytically and the center-of-mass trajectory becomes a circle ($T = 0$) or a logarithmic spiral ($T > 0$) like in Ref. [39]. The analytical solution for $U(\vec{r}, \phi) = f_\parallel = f_\perp = \tau = 0$ is given by

$$\begin{aligned}\vec{r}(t) &= \vec{r}_0 + \frac{\beta}{\omega}(F_{\parallel}D_2 + F_{\perp}D_3 - MD_C^{\perp})(\hat{u}_{\parallel}(\phi_0 + \omega t) - \hat{u}_{\parallel}(\phi_0)) \\ &\quad - \frac{\beta}{\omega}(F_{\parallel}D_1 + F_{\perp}D_2 - MD_C^{\parallel})(\hat{u}_{\perp}(\phi_0 + \omega t) - \hat{u}_{\perp}(\phi_0)), \\ \phi(t) &= \phi_0 + \omega t\end{aligned}\quad (31)$$

$$\phi(t) = \phi_0 + \omega t \quad (32)$$

with the angular velocity

$$\omega = \beta(MD_R - D_C^{\parallel}F_{\parallel} - D_C^{\perp}F_{\perp}), \quad (33)$$

the initial position $\vec{r}_0 = \vec{r}(0)$, and the initial orientation $\phi_0 = \phi(0)$. If instead of $U(\vec{r}, \phi)$ the translational diffusion coefficient D_2 and the coupling coefficients D_C^{\parallel} and D_C^{\perp} vanish, as is the case for a particle with double inflection symmetry, the Langevin equations (19) become similar to the Langevin equations for the Brownian circle swimmer in Ref. [39], but with a more general driving force \vec{F}_A , which is not necessarily parallel to the figure axis. For $D_2 = D_C^{\parallel} = D_C^{\perp} = F_{\perp} = 0$, the Langevin equations (19) are equivalent to the Langevin equation in Ref. [39]. An additional constraint on spherical particles, which are able only to move along the x_1 axis, leads to the Langevin equations for a spherical self-propelled particle on a substrate [40]. With similar simplifications it is also possible to obtain the Langevin equations for spherical or anisotropic uniaxial self-propelled particles in two spatial dimensions, which are discussed in Ref. [41], from Eqs. (19).

C. Orthotropic particles

Another possibility to simplify the Langevin equation (1) considerably is the exclusive consideration of orthotropic particles. All geometric bodies with three pairwise orthogonal planes of symmetry like spheres, spheroids (ellipsoids of revolution), biaxial (or triaxial) ellipsoids, cylinders, cuboids, and some prisms belong to this important class. Orthotropic particles have no translational-rotational coupling so that the coupling tensor C_S vanishes. Furthermore, the translation tensor K and the rotation tensor Ω_S are diagonal for orthotropic particles. These properties of K , C_S , and Ω_S can be derived from the circumstance that the center of mass, which should be chosen as reference point S , and the mutual point of intersection of the three planes of symmetry of an orthotropic particle coincide [52]. The vanishing of the coupling tensor C_S results from the fact that the point of intersection of the three pairwise perpendicular planes of symmetry of the particle is identical with the *center of hydrodynamic reaction* for orthotropic bodies. With these considerations, the Langevin equation (1) simplifies to the *Langevin equations for orthotropic particles*:

$$\begin{aligned}\dot{\vec{r}} &= \beta D^{TT}(\vec{\omega})[R^{-1}(\vec{\omega})\vec{F}_0 - \vec{\nabla}_{\vec{r}}U + R^{-1}(\vec{\omega})\vec{k}_1], \\ \dot{\vec{\omega}} &= \beta D^{RR}(\vec{\omega})[R^{-1}(\vec{\omega})\vec{T}_0 - \vec{\nabla}_{\vec{\omega}}U + R^{-1}(\vec{\omega})\vec{k}_2] \\ &\quad + \vec{\nabla}_{\vec{\omega}} \cdot D^{RR}(\vec{\omega}).\end{aligned}\quad (34)$$

Here the Gaussian white noises \vec{k}_1 and \vec{k}_2 are independent and defined as the first and second parts of $\vec{k} = (\vec{k}_1, \vec{k}_2)$, respectively. The Langevin equations for spherical or uniaxial particles, which are considered in Ref. [41], are special cases

of the more general Langevin equations (34) for biaxial orthotropic particles. To be able to solve these Langevin equations analytically, it is at first necessary to neglect \vec{k}_1 and \vec{k}_2 , i.e., to consider the case $T = 0$. A further negligence of the drive or the external potential leads to two special cases, which are analytically solvable.

1. Settling orthotropic passive particle

A particle without drive, i.e., with $\vec{F}_0 = \vec{T}_0 = \vec{0}$, at $T = 0$ moves only under the influence of the external potential $U(\vec{r}, \vec{\omega})$ at $T = 0$. In the case of a constant gravitational field, only the constant external force $\vec{F}_{\text{ext}} = -\vec{\nabla}_{\vec{r}}U$ acts on the particle and the external torque $-\vec{\nabla}_{\vec{\omega}}U$ vanishes. The motion of such a sedimenting particle is well known from the literature [52]. It is characterized by a constant velocity $\dot{\vec{r}}$ and a constant orientation $\vec{\omega}$:

$$\dot{\vec{r}} = \beta D^{TT}(\vec{\omega}_0)\vec{F}_{\text{ext}} = \text{const}, \quad \vec{\omega} = \vec{\omega}_0 = \text{const}. \quad (35)$$

2. Self-propelled orthotropic particle

If the external potential $U(\vec{r}, \vec{\omega})$ is neglected instead of the drive in Eqs. (34) for $T = 0$, they describe the helical motion of an arbitrary orthotropic self-propelled particle in the absence of external and random forces and torques:

$$\dot{\vec{r}} = R^{-1}(\vec{\omega})K^{-1}\frac{1}{\eta}\vec{F}_0, \quad \dot{\vec{\omega}} = R^{-1}(\vec{\omega})\Omega_S^{-1}\frac{1}{\eta}\vec{T}_0. \quad (36)$$

These equations of motion are trivial in the body-fixed coordinate system, where the velocities $\dot{\vec{r}}$ and $\dot{\vec{\omega}}$ are constant. Since the angular velocity $\vec{\omega}$ with the initial orientation $\vec{\omega}_0 = \vec{\omega}(0)$ is constant in body-fixed coordinates, it is also constant in the space-fixed system. This means that one expects a helix for the center-of-mass trajectory as is known from the motion of protozoa like *Euglena gracilis* [38] and bacteria like *Thiovulum majus* [48]. The analytical solution of Eqs. (36) is in fact the circular helix

$$\begin{aligned}\vec{r}(t) &= \vec{r}_0 + \frac{(\vec{\omega} \times \vec{v}_0) \times \vec{\omega}}{|\vec{\omega}|^3} \sin(|\vec{\omega}|t) \\ &\quad + \frac{\vec{\omega} \times \vec{v}_0}{|\vec{\omega}|^2} [1 - \cos(|\vec{\omega}|t)] + \frac{\vec{\omega} \cdot \vec{v}_0}{|\vec{\omega}|^2} \vec{\omega}t\end{aligned}\quad (37)$$

with axis

$$\mathbb{A} = \vec{r}_0 + \frac{\vec{\omega} \times \vec{v}_0}{|\vec{\omega}|^2} + \vec{\omega}\mathbb{R} \quad (38)$$

along $\vec{\omega}$, radius

$$r = \frac{|(K^{-1}\vec{F}_0) \times (\Omega_S^{-1}\vec{T}_0)|}{\eta^2|\vec{\omega}|^2}, \quad (39)$$

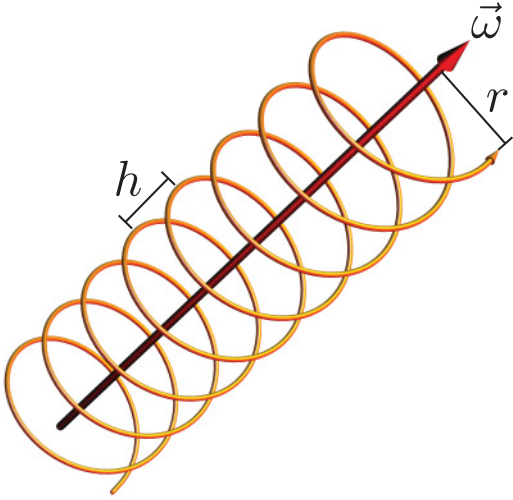


FIG. 1. (Color online) The center-of-mass trajectory of an orthotropic particle for a constant external potential and $T = 0$ is a circular helix with radius r and pitch h , which evolves from the rotation of the orthotropic particle with the constant angular velocity $\vec{\omega}$.

and pitch

$$h = 2\pi \frac{|(\mathbf{K}^{-1}\vec{F}_0) \cdot (\Omega_S^{-1}\vec{T}_0)|}{\eta^2|\vec{\omega}|^2}, \quad (40)$$

where $\vec{r}_0 = \vec{r}(0)$ is the initial position, $\vec{v}_0 = \dot{\vec{r}}(0) = \mathbf{R}^{-1}(\vec{\omega}_0)\mathbf{K}^{-1}\vec{F}_0/\eta$ is the initial velocity, and $|\vec{\omega}| = |\Omega_S^{-1}\vec{T}_0/\eta|$ is the modulus of the angular velocity. This helical trajectory is shown schematically in Fig. 1. When a constant gravitational field also is taken into account, the helix becomes deformed, and, for example, its cross section might become elliptic, but the axis of the helix remains a straight line. In the case $T > 0$, where we have to consider the stochastic contributions in the Langevin equations (34), it is, however, no longer possible to find analytical solutions. This case requires the usage of appropriate numerical integrators for stochastic differential equations and is studied in the next paragraph.

IV. NUMERICAL CALCULATIONS

In general situations, where analytical solutions do not exist, the Langevin equation (1) can be investigated only with the help of numerical methods. Appropriate numerical methods in increasing order of the truncation error are the Euler-Maruyama method, Milstein method, and stochastic Runge-Kutta methods [56], which have to be derived in the Itô sense in order to be compatible with the Langevin equations in this paper. If there are no thermal fluctuations ($T = 0$), the stochastic Langevin equation (1) becomes deterministic and a standard Runge-Kutta scheme of high order can be applied.

The numerical results for $T = 0$ and $T > 0$, which are presented in the following, have been obtained with an explicit fourth-order deterministic Runge-Kutta scheme [57–60] and with a multidimensional explicit stochastic Runge-Kutta scheme of weak order 2.0 for Itô stochastic differential equations [56], respectively. This stochastic Runge-Kutta scheme was chosen for the numerical solution of the Langevin equations in this paper, since it has a higher order than the

most other schemes for numerical stochastic integration and since it is simple to use. Through its multidimensionality, it can directly be applied simultaneously to a system of coupled stochastic differential equations, and since this scheme is explicit, the computational effort for one evaluation is rather small. Implicit schemes are in contrast computationally much more expensive. The application of an implicit scheme is in general necessary, if a stiff stochastic differential equation has to be solved, which is not the case here. Furthermore, the chosen stochastic Runge-Kutta scheme does not involve the evaluation of time derivatives of parts of the stochastic differential equation, which would have to be approximated numerically in turn. This is very convenient and a general feature of Runge-Kutta schemes. More information about numerical methods for the solution of stochastic differential equations is described in Ref. [56].

In the whole section, \vec{F}_0 , \vec{T}_0 , $\vec{F}_{\text{ext}} = -\vec{\nabla}_{\vec{r}}U$, and $\vec{T}_{\text{ext}} = -\vec{\nabla}_{\vec{\omega}}U$ are assumed to be constant vectors, which do not depend on \vec{r} or $\vec{\omega}$. Furthermore, arbitrary Brownian particles with a hydrodynamic translational-rotational coupling and orthotropic particles without a translational-rotational coupling in two and three spatial dimensions are considered for $T = 0$ and $T > 0$. In parallel to the previous section, this section is divided into a first subsection about the general Langevin equation for three spatial dimensions, a second subsection about two spatial dimensions, and a third subsection about orthotropic particles.

A. Three spatial dimensions

For arbitrarily shaped particles in three spatial dimensions, one finds various differently shaped trajectories as solutions of the Langevin equation (1). Figure 2 gives a selection of typical trajectories that can be observed for arbitrarily shaped particles with an arbitrary drive at $T = 0$. In order to sample some typical solutions, we have randomly chosen the 21 shape-dependent parameters for the matrix \mathcal{H} , the components of the internal force \vec{F}_0 and torque \vec{T}_0 , the components of the external force \vec{F}_{ext} and torque \vec{T}_{ext} , and the initial conditions. More than 100 random parameter combinations were considered. In doing so, four different cases with vanishing and nonvanishing vectors for \vec{F}_{ext} and \vec{T}_{ext} were distinguished (see Fig. 2). Depending on the choice of \vec{F}_{ext} and \vec{T}_{ext} , the observed trajectories appeared to share features and to be distinguishable into four different classes. The four trajectories that are shown in Fig. 2 are representatives of these classes. They can be characterized as follows: If there are both an external force and an external torque, self-propelled particles that start with an irregular transient regime and end up in a simple periodic center-of-mass trajectory are usually observed [see Fig. 2(a)]. Note that the length of the initial transient regime as well as the periodicity length of the final periodic motion depend on the particular parameters and may become rather long. In the case of no external torque, the periodic motion after the transient regime is a circular helix with its axis being parallel to the direction of the external force vector. This situation is illustrated in Fig. 2(b). The analog case of an external torque but no external force is schematically shown in Fig. 2(c). There a *superhelix*-like curve with the orientation parallel to the direction of the external torque vector and without a preceding

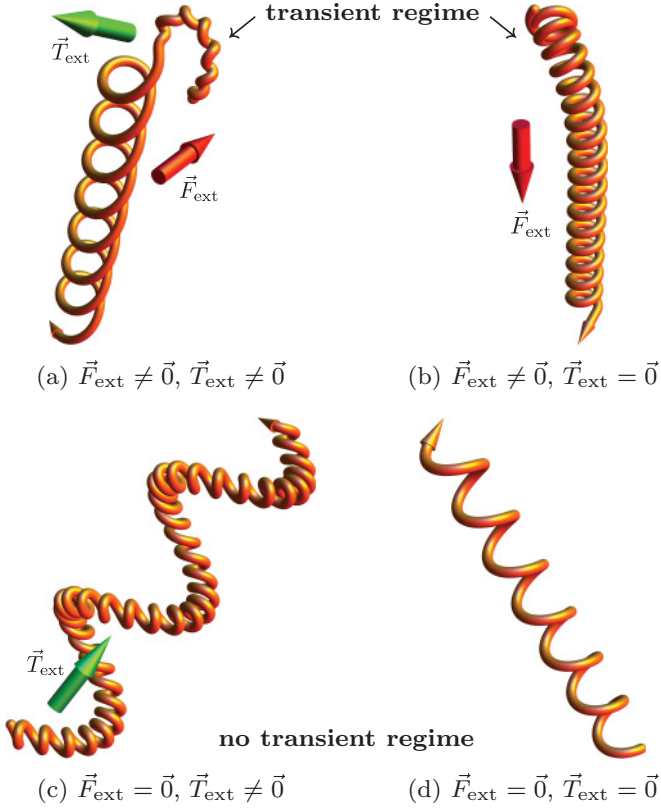


FIG. 2. (Color online) Typical trajectories of arbitrarily shaped active particles in three spatial dimensions for constant vectors $\vec{F}_0 \neq \vec{0}$, $\vec{T}_0 \neq \vec{0}$, and temperature $T = 0$. The external force $\vec{F}_{\text{ext}} = -\vec{\nabla}_{\vec{r}}U$ and torque $\vec{T}_{\text{ext}} = -\vec{\nabla}_{\vec{\theta}}U$ are constant too. For a nonvanishing external force, the particle's center-of-mass trajectory starts with an irregular transient regime and changes into a periodic motion, as is shown in plots (a) and (b). The general periodic motion (a), which is observed if there is also a nonvanishing external torque, reduces to a circular helix (b) parallel to the external force if there is no external torque. The other two plots (c) and (d) show the situation for a vanishing external force, where a transient regime is not observed. There, the trajectory is either a *superhelix*-like curve (c) parallel to a nonvanishing external torque or a circular helix (d) if there is no external torque. However, the trajectories (a)–(c) can also be irregular. Straight trajectories, which are preceded by a transient regime for $\vec{F}_{\text{ext}} \neq \vec{0}$, can be observed too.

transient regime is observed. In contrast to the trajectory in Fig. 2(a), the complicated superhelix-like curve does not turn into a simpler periodic curve after some time, since there is no transient regime for $\vec{F}_{\text{ext}} = \vec{0}$. As a fourth case, the motion in the absence of both external forces and torques is shown in Fig. 2(d). It appears to be a circular helix. Also in this case, a transient regime is not observed. In the situation of Fig. 2(a) and 2(b), completely irregular trajectories can appear, when the transient regime is very long. Even in the transient-free situation of Fig. 2(c), irregular trajectories are observed, when the rotational frequency ratio between the immanent rotation of the self-propelled particle and the rotation due to the external torque is irrational. Furthermore, straight trajectories appear as a special case. They are preceded by a transient regime if $\vec{F}_{\text{ext}} \neq \vec{0}$. A complete and detailed classification of

all trajectories that can be observed in three spatial dimensions is, however, not possible, since the number of the parameters that define the shape of the particle and all further relevant quantities like internal and external forces and torques is quite big, but this number is much smaller in two spatial dimensions, where a more detailed classification is possible.

B. Two spatial dimensions

The Langevin equations (19) for two spatial dimensions were solved analytically in Sec. III B for $U(\vec{r}, \phi) = 0$ and $T = 0$. Here we consider the case $T = 0$ too, but now for a constant nonvanishing external force $\vec{F}_{\text{ext}} = -\vec{\nabla}_{\vec{r}}U$, since the external force leads to various different nontrivial trajectories. The observed trajectories are classified with respect to the shape and the kind of self-propulsion of the particle in Table II. Since the drift coefficients B_1^{\parallel} and B_1^{\perp} can be neglected for $T = 0$, the shape of the particle is described only with the six parameters D_1 , D_2 , D_3 , D_C^{\parallel} , D_C^{\perp} , and D_R , where D_1 and D_R can be set to one by a suitable rescaling of the length and time scales. For the remaining parameters, particles with a translational-rotational coupling and particles without a translational-rotational coupling as well as asymmetric particles, particles with one axis of symmetry, particles with two mutually perpendicular axes of symmetry, and isotropic particles with rotational symmetry are distinguished. Moreover, the constant parameters F_{\parallel} , F_{\perp} , and $M_{\text{eff}} = M - \partial_{\phi}U$ are used to describe the self-propulsion of the particle. Four situations of a nonvanishing internal force \vec{F}_A and torque M , a drive only by either an internal force or an internal torque, and a passive particle with a vanishing drive are considered. A further distinction with respect to the external force and torque is not necessary, because the external force can always be chosen bigger than zero, since the case of a vanishing external force has been proven to lead to a trivial circular trajectory in Sec. III B, and the external torque $-\partial_{\phi}U$ is already included in the effective torque M_{eff} and can be neglected. In general, straight lines with an aperiodic transient regime, arbitrary periodic curves, cycloids, and simple straight lines were found as trajectories in two spatial dimensions by random choices of the parameters. These trajectories still have the basic features of their three-dimensional analogs, but are much simpler to describe. It is only for particles with translational-rotational coupling, i.e., particles where at least one of the coefficients D_C^{\parallel} and D_C^{\perp} does not vanish, that the straight trajectories are preceded by an initial transient regime. These trajectories are characterized by a monotonous rotation of the particle when it starts moving and an ensuing rotation-free straight motion. In the transient regime, the particle rotates until the internal torque, the external torque, and the additional torque due to the translational-rotational coupling compensate each other. For active particles with translational-rotational coupling, periodic trajectories also are observed, where a canceling of the total torque does not happen during the initial rotation. This is not the case for symmetric particles with a vanishing effective torque M_{eff} and for passive particles, for which a periodic trajectory is not observed. The motion of symmetric particles without translational-rotational coupling is always periodic or constant. In both cases, the trajectory is parallel to the direction of the external force, if the

TABLE II. (Color online) Detailed classification of the trajectories of arbitrarily shaped particles in two spatial dimensions for $T = 0$ with respect to the symmetries that are summarized in Table I. For the external force, $\vec{F}_{\text{ext}} \neq \vec{0}$ is chosen, since all trajectories become circles otherwise. In the plots below, \vec{F}_{ext} is always oriented downward, i.e., in the negative x_2 direction. Internal and external torque are combined to the effective torque $M_{\text{eff}} = M - \partial_\phi U$.

particle shape	no symmetry	x_1 -axis or x_2 -axis is axis of symmetry	x_1 -axis and x_2 -axis are axes of symmetry	rotational symmetry
	$D_2 \neq 0, D_3 \neq 0,$ $D_C^\parallel \neq 0, D_C^\perp \neq 0$	$D_2 = 0, D_3 \neq 0,$ $D_C^\parallel \neq 0 \vee D_C^\perp \neq 0$	$D_2 = 0, D_3 \neq 0,$ $D_C^\parallel = 0, D_C^\perp = 0$	$D_2 = 0, D_3 = D_1,$ $D_C^\parallel = 0, D_C^\perp = 0$
$F_\parallel \neq 0, F_\perp \neq 0, M_{\text{eff}} \neq 0$				
	straight line after transient regime ^a or periodic curve ^b	straight line after transient regime ^a or periodic curve ^b	periodic curve ^c $\parallel \vec{F}_{\text{ext}}$	cycloid ^c $\parallel \vec{F}_{\text{ext}}$
$F_\parallel \neq 0, F_\perp \neq 0, M_{\text{eff}} = 0$				
	straight line after transient regime ^a or periodic curve ^b	straight line after transient regime ^a	straight line ^d	straight line ^d
$F_\parallel = 0, F_\perp \neq 0, M_{\text{eff}} \neq 0$				
	straight line after transient regime ^a or periodic curve ^b	str. line after trans. regime ^a or periodic curve ^b $\parallel \vec{F}_{\text{ext}}$	cycloid ^c $\parallel \vec{F}_{\text{ext}}$	straight line ^c $\parallel \vec{F}_{\text{ext}}$
$F_\parallel = 0, F_\perp = 0, M_{\text{eff}} = 0$				
	straight line after transient regime ^a	straight line after transient regime ^a $\parallel \vec{F}_{\text{ext}}$	straight line ^d	straight line ^d $\parallel \vec{F}_{\text{ext}}$

^aThe particle rotates monotonously until it reaches its final orientation. Then the angle ϕ remains constant.

^bThe angle ϕ and the center of mass of the particle describe periodic curves with the same periodicity.

^cThe particle rotates with a constant angular velocity, i.e., $\phi \propto t$.

^dThe orientation of the particle is constant: $\phi = \text{const.}$

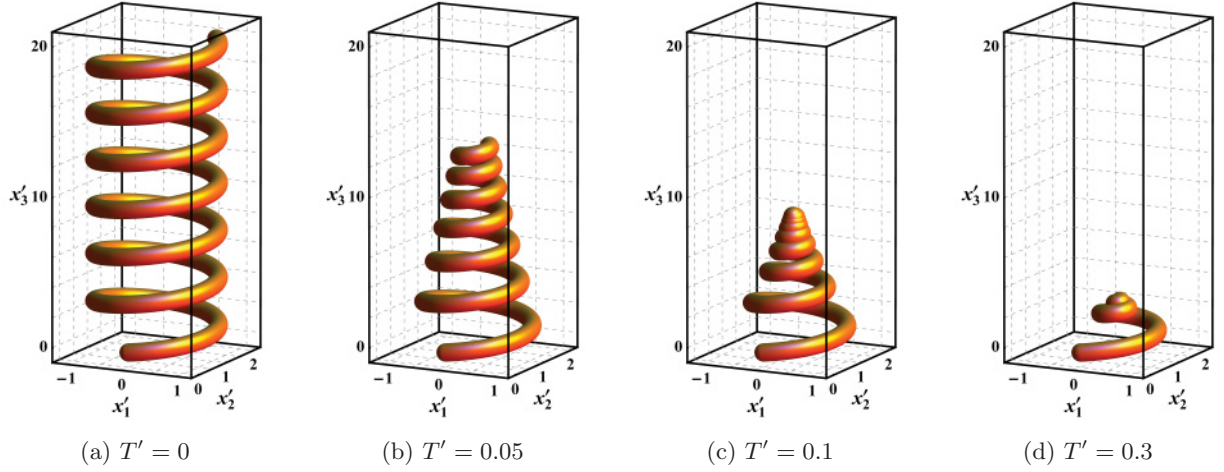


FIG. 3. (Color online) Mean trajectories of a self-propelled orthotropic particle in the absence of external forces and torques for the dimensionless temperatures $T' = 0$, $T' = 0.05$, $T' = 0.1$, and $T' = 0.3$. In the left two plots, the trajectories are shown for the time interval $0 \leq t' \leq 40$, while the right two plots show mean trajectories with $0 \leq t' \leq 80$.

effective torque M_{eff} is not zero. Without the effective torque, only straight trajectories are observed for these particles. Solely in the case of passive rotationally symmetric particles, the orientation of these straight trajectories is parallel to the external force.

C. Orthotropic particles

To regard the influence of thermal fluctuations on the motion of a biaxial self-propelled Brownian particle, the Langevin equations (34) for orthotropic particles are solved numerically for $T > 0$ in this section. For this purpose, first, characteristic quantities for the length scale, time scale, and force scale are chosen, and the Langevin equations (34) are rescaled to dimensionless units. A suitable choice for the characteristic length l_c , the characteristic time t_c , and the characteristic force F_c is

$$l_c = \sqrt{\frac{\lambda_{\max}(\mathbf{D}^{\text{TT}})}{\lambda_{\max}(\mathbf{D}^{\text{RR}})}}, \quad (41)$$

$$t_c = \frac{1}{\lambda_{\max}(\mathbf{D}^{\text{RR}})}, \quad (42)$$

$$F_c = \frac{\eta l_c^2}{t_c} = \eta \lambda_{\max}(\mathbf{D}^{\text{TT}}), \quad (43)$$

where $\lambda_{\max}(\cdot)$ denotes the biggest eigenvalue of the respective matrix. These characteristic quantities are used to express the position $\vec{r} = \vec{r}' l_c$, time $t = t' t_c$, forces $\vec{F}_0 = \vec{F}'_0 F_c$, $\vec{F}_{\text{ext}} = \vec{F}'_{\text{ext}} F_c$, torques $\vec{T}_0 = \vec{T}'_0 F_c l_c$, $\vec{T}_{\text{ext}} = \vec{T}'_{\text{ext}} F_c l_c$, translation tensor $\mathbf{K} = \mathbf{K}' l_c$, and rotation tensor $\Omega_S = \Omega'_S l_c^3$ by the dimensionless position $\vec{r}' = (x'_1, x'_2, x'_3)$, time t' , forces \vec{F}'_0 , \vec{F}'_{ext} , torques \vec{T}'_0 , \vec{T}'_{ext} , translation tensor \mathbf{K}' , and rotation tensor Ω'_S , respectively. In the rescaled Langevin equations, the parameter

$$T' = \frac{2t_c}{\eta\beta l_c^3} = \frac{2}{\eta\beta} \sqrt{\frac{\lambda_{\max}(\mathbf{D}^{\text{RR}})}{\lambda_{\max}^3(\mathbf{D}^{\text{TT}})}} \propto T \quad (44)$$

appears as a dimensionless temperature. This parameter is varied and fluctuation-averaged trajectories are calculated for different temperatures with fixed initial conditions \vec{r}'_0

and $\vec{\omega}'_0$. The results for the case of vanishing external forces and torques, where the trajectory for $T' = T = 0$ is known from the analytical solution in Sec. III C to be a circular helix, are shown in Fig. 3. For this figure we chose the dimensionless forces $\vec{F}'_0 = (-0.5, 0, 3)$, $\vec{F}'_{\text{ext}} = \vec{0}$, torques $\vec{T}'_0 = (-1, 0, 0)$, $\vec{T}'_{\text{ext}} = \vec{0}$, translation tensor $\mathbf{K}' = \text{diag}(1, 2, 3)$, rotation tensor $\Omega'_S = \text{diag}(1, 3, 4)$, initial conditions $\vec{r}'_0 = (x'_{1,0}, x'_{2,0}, x'_{3,0}) = \vec{0}$, $\vec{\omega}'_0 \equiv \vec{\omega}_0 = (0, \pi/2, 0)$, and temperatures $T' = 0, 0.05, 0.1, 0.3$. It is apparent that the center-of-mass trajectory for $T' = 0$ and the fluctuation-averaged center-of-mass trajectories for $T' > 0$ have no transient regime in Fig. 3. This is also the case for nonvanishing constant external forces and torques and a general feature of orthotropic particles in contrast to less symmetric particles with a translational-rotational coupling. In the presence of thermal fluctuations, the helical motion of the self-propelled orthotropic particle is damped exponentially with time, and the fluctuation-averaged center-of-mass trajectory becomes a *concho-spiral* [49], whose radius and pitch decay exponentially with time [see Figs. 4(a) and 4(b)]. This result was confirmed by a fit of the numerical solutions with the general parametrization of a concho-spiral and agrees with the observation of a logarithmic spiral, also named *spira mirabilis* by Jacob Bernoulli, in the two-dimensional special case of our Langevin equations, which is investigated in Ref. [39]. In the situation of Fig. 3, the axes of the concho-spirals are parallel to the x'_3 axis and can be parametrized by [39,49]

$$x'_1(t') = x'_{1,0} + \alpha'_1 \{\cos(\phi_0) - \cos[\phi(t')]\} e^{-\gamma'_1 t'} - \alpha'_2 \{\sin(\phi_0) - \sin[\phi(t')]\} e^{-\gamma'_1 t'}, \quad (45)$$

$$x'_2(t') = x'_{2,0} + \alpha'_1 \{\sin(\phi_0) - \sin[\phi(t')]\} e^{-\gamma'_1 t'} + \alpha'_2 \{\cos(\phi_0) - \cos[\phi(t')]\} e^{-\gamma'_1 t'}, \quad (46)$$

$$x'_3(t') = x'_{3,0} + H'_{\max} [1 - (1 - \varepsilon' t') e^{-\gamma'_2 t'}], \quad (47)$$

$$\phi(t') = \phi_0 + \omega' t' \quad (48)$$

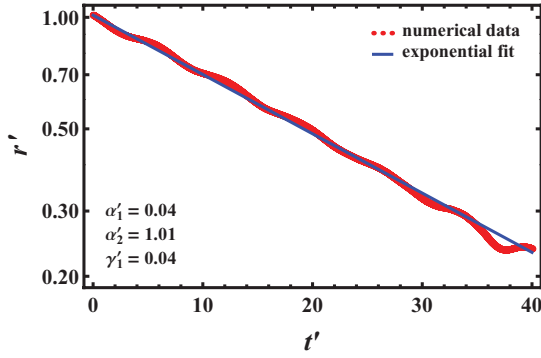
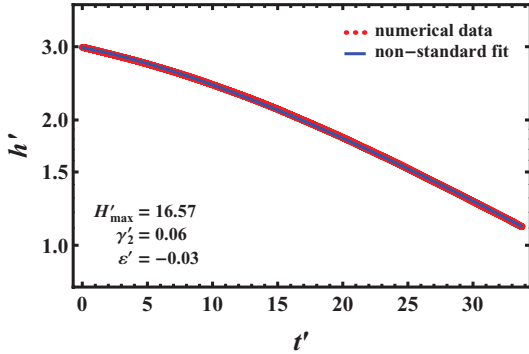
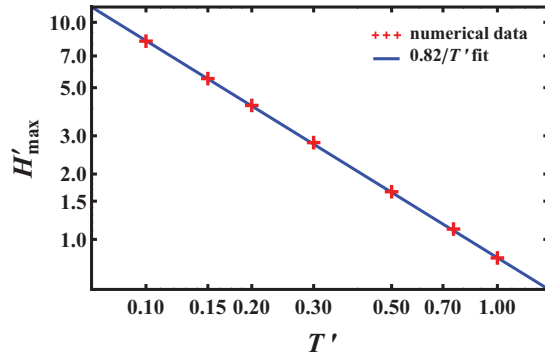

 (a) radius $r'(t') = r(t)/l_c$

 (b) pitch $h'(t') = h(t)/l_c$

 (c) height $H_{\max}'(T') = H_{\max}(T)/l_c$

FIG. 4. (Color online) (a) Radius and (b) pitch of a trajectory that is shaped as a concho-spiral decay exponentially with time t' . In the linear-logarithmic plots (a) and (b), the exponential decay is obvious for the radius, but not for the pitch, where the exponential function has a linear time-dependent prefactor [see Eq. (51)]. The numerical data (red dots following a curved line) for these plots were taken from the concho-spiral in Fig. 3(b). (c) The height of the concho-spirals is inversely proportional to the temperature T' . The parameters for plot (c) are the same as in Fig. 3, but with more and different values for T' . In each plot, a blue line corresponding to Eqs. (49)–(52) was fitted to the numerical data.

with the angular frequency $\omega' = |\vec{\omega}'| = |\Omega_S^{-1} \vec{T}'_0|$ [see Eqs. (36)] and the dimensionless fit parameters α'_1 , α'_2 , γ'_1 , γ'_2 , H'_{\max} , and ε' . Equations (45), (46), and (48) describe a logarithmic spiral, which is the trajectory of the two-dimensional circle swimmer in Ref. [39], while the parametrization (47) of the third spatial variable $x'_3(t')$ is here more general than

in Ref. [49]. In Eq. (47) there is an additional term $\propto \varepsilon'$, which makes sure that a helix is obtained as a special case of the concho-spiral for $T' = 0$, i.e., for $\gamma'_1 = \gamma'_2 = 0$. This is, however, not the case for the parametrization in Ref. [49]. Based on the parametrization (45)–(48), radius and pitch of the concho-spirals can be derived. The fit parameters α'_1 , α'_2 , and γ'_1 determine the dimensionless radius $r'(t') = r(t)/l_c$ of the concho-spirals:

$$r'(t') = r'_0 e^{-\gamma'_1 t'}, \quad (49)$$

$$r'(0) = r'_0 = \sqrt{\alpha_1'^2 + \alpha_2'^2}. \quad (50)$$

Their dimensionless pitch $h'(t') = h(t)/l_c$ depends on the remaining fit parameters γ'_2 , H'_{\max} , and ε' :

$$h'(t') = H'_{\max} e^{-\gamma'_2 t'} \left[(1 - \varepsilon' t') \left(1 - e^{-\frac{2\pi}{\omega'} \gamma'_2} \right) + \varepsilon' \frac{2\pi}{\omega'} e^{-\frac{2\pi}{\omega'} \gamma'_2} \right]. \quad (51)$$

Numerical values for radius and pitch are shown in Figs. 4(a) and 4(b). Furthermore, the height $H_{\max}(T)$ of the concho-spiral and its dimensionless analog $H'_{\max}(T') = H_{\max}(T)/l_c$, defined as the distance from the initial position of the particle to its final position for $t' \rightarrow \infty$ measured along the axis of the concho-spiral, are finite and decrease monotonously, when the temperature is increased. For the numerical calculations that correspond to the results shown in Fig. 3, the inverse power law

$$H'_{\max}(T') \approx 0.82 T'^{-1} \quad (52)$$

was determined [see Fig. 4(c)]. When there is additionally a constant external force, the helix for $T' = 0$ as well as the concho-spirals for $T' > 0$ are deformed, and their cross sections can become elliptic.

V. CONCLUSIONS AND OUTLOOK

In conclusion, we have studied the Langevin equation governing the motion of a driven Brownian spinning top describing a self-propelled biaxial colloidal particle. The particle is driven by both internal and external forces and torques, which are constant in the body frame and in the laboratory frame, respectively. This equation is nontrivial due to the geometric biaxiality and the hydrodynamic translational-rotational coupling of the particle and can therefore only be solved numerically. In the special case of an orthotropic particle in the absence of external forces and torques, the noise-free trajectory is analytically found to be a circular helix, and the noise-averaged trajectory is a generalized *concho-spiral*. The noise-free trajectory is confirmed numerically to be more complex for a translational-rotational coupling involving a transient irregular motion before ending up in a simple periodic motion. By contrast, if the external force vanishes, no transient is found and the particle moves on a *superhelical* trajectory. We furthermore studied in detail the much simpler reduction of the model to two spatial dimensions. In two spatial dimensions, the noise-free trajectories are classified completely, and circles, straight lines with and without transients, as well as cycloids and arbitrary periodic trajectories are found.

The Langevin equation derived here can be used as a starting point to describe more complex situations. As examples, we mention a particle in confinement of linear channels [24,34,61] or cylindrical tubes [27,62]. A sliding motion can be expected similar as in the two-dimensional reduction of our model [39]. In confinement, details of the propulsion mechanism are getting relevant since they result in different hydrodynamic interactions of the particle with the system boundaries [63].

A next level of complexity is given by an ensemble of swimmers, i.e., a finite number density, which can interact either directly by excluded volume or via hydrodynamic interactions. Recently a dynamical density functional theory has been proposed for biaxial particles [64] following the lines given for uniaxial particles [65]. The collective properties of self-propelled biaxial particles are assumed to be rich, including turbulent states, swarming, and jamming [66,67].

Finally, one can impose a nonvanishing solvent flow, like Couette shear flow [68], and study a self-propelled particle there [69]. Our Langevin equation can be straightforwardly generalized to this situation [45] and may lead to new shear-induced tumbling phenomena of self-propelled biaxial particles.

ACKNOWLEDGMENTS

We thank Gerhard Nägele, Ludger Harnau, Gerrit Jan Vroege, Holger Stark, Henricus H. Wensink, Michael Schmiedeberg, Borge ten Hagen, and Reinhard Vogel for helpful discussions. This work has been supported by SFB TR6 (project D3).

APPENDIX: DERIVATION OF THE LANGEVIN EQUATION

In this appendix, we provide more details to derive the Langevin equation (1). There are four forces and four torques that act on the self-propelled Brownian particle. In the laboratory frame, these forces and torques are the internal force \vec{F}_{int} and torque \vec{T}_{int} , the external force $\vec{F}_{\text{ext}} = -\vec{\nabla}_{\vec{r}}U$ and torque $\vec{T}_{\text{ext}} = -\vec{\nabla}_{\vec{\omega}}U$ due to the external potential $U(\vec{r})$, the hydrodynamic friction force \vec{F}_{H} and torque \vec{T}_{H} , and the Brownian force \vec{F}_{Br} and torque \vec{T}_{Br} due to thermal fluctuations. The internal force and torque can be represented by constant vectors \vec{F}_0 and \vec{T}_0 in the body-fixed frame, respectively, and are

given by $\vec{F}_{\text{int}} = \mathbf{R}^{-1}(\vec{\omega})\vec{F}_0$ and $\vec{T}_{\text{int}} = \mathbf{R}^{-1}(\vec{\omega})\vec{T}_0$ in the space-fixed frame, respectively. Since the Reynolds number of the considered system is very small, low Reynolds number hydrodynamics can be applied to determine the hydrodynamic friction force and torque. They are given as linear functions of the translational velocity $\vec{r}(t)$ and angular velocity $\vec{\omega}$ through [52]

$$\begin{aligned}\vec{F}_{\text{H}} &= -\eta[\mathbf{R}^{-1}(\vec{\omega})\mathbf{K}\mathbf{R}(\vec{\omega})\dot{\vec{r}} + \mathbf{R}^{-1}(\vec{\omega})\mathbf{C}_{\text{S}}^{\text{T}}\mathbf{R}(\vec{\omega})\vec{\omega}], \\ \vec{T}_{\text{H}} &= -\eta[\mathbf{R}^{-1}(\vec{\omega})\mathbf{C}_{\text{S}}\mathbf{R}(\vec{\omega})\dot{\vec{r}} + \mathbf{R}^{-1}(\vec{\omega})\Omega_{\text{S}}\mathbf{R}(\vec{\omega})\vec{\omega}],\end{aligned}\quad (\text{A1})$$

where the rotation matrix $\mathbf{R}^{-1}(\vec{\omega})$ again transforms body-fixed coordinates into space-fixed coordinates. Finally, the Brownian force and torque are characterized by the stochastic force $\vec{f}_0(t)$ and torque $\vec{\tau}_0(t)$. These two stochastic noise vectors describe random forces and torques due to thermal fluctuations in the body-fixed frame. In terms of $\vec{f}_0(t)$ and $\vec{\tau}_0(t)$, the Brownian force and torque can be written as $\vec{F}_{\text{Br}} = \mathbf{R}^{-1}(\vec{\omega})\vec{f}_0 + \vec{F}_{\text{D}}$ and $\vec{T}_{\text{Br}} = \mathbf{R}^{-1}(\vec{\omega})\vec{\tau}_0 + \vec{T}_{\text{D}}$ with the additional contributions \vec{F}_{D} and \vec{T}_{D} , which are determined later.

The overdamped Brownian particle is force free and torque free [1]. With the notation $\vec{K}_{\dots} = (\vec{F}_{\dots}, \vec{T}_{\dots})$, this condition can be expressed by

$$\vec{K}_{\text{A}} + \vec{K}_{\text{int}} + \vec{K}_{\text{ext}} + \vec{K}_{\text{Br}} = \vec{0}. \quad (\text{A2})$$

This is equivalent to the Langevin equation

$$\dot{\vec{v}} = \beta\mathcal{D}(\vec{r})[\mathcal{R}^{-1}(\vec{r})\vec{K}_0 - \vec{\nabla}_{\vec{r}}U(\vec{r}) + \mathcal{R}^{-1}(\vec{r})\vec{k}] + \vec{B}(\vec{r}) \quad (\text{A3})$$

with $\vec{B}(\vec{r}) = \beta\mathcal{D}(\vec{r})\vec{K}_{\text{D}}$. The vectors $\vec{k}(t)$ and $\vec{B}(\vec{r})$ have still to be defined. To do so, the stochastic noise $\vec{k}(t)$ is assumed to be the equilibrium Gaussian white noise, which acts on the Brownian particle for $T > 0$. As a consequence of the general fluctuation-dissipation theorem, the noise $\vec{k}(t)$ is then defined by Eqs. (15) and (16). The additional drift term $\vec{B}(\vec{r})$ has to be taken into account to ensure that the definition of the Langevin equation (A3) is consistent with the Boltzmann distribution in thermodynamic equilibrium. It can be determined with the help of the Smoluchowski equation, which is equivalent to the Langevin equation (A3). A comparison of the equilibrium special case with $\vec{K}_0 = \vec{0}$ of this Langevin equation with the Boltzmann distribution [1,53] leads to $\vec{B}(\vec{r}) = \vec{\nabla}_{\vec{r}} \cdot \mathcal{D}(\vec{r})$ and states that Eq. (A3) is equivalent to the Langevin equation (1).

-
- [1] J. K. G. Dhont, *An Introduction to Dynamics of Colloids*, Studies in Interface Science, Vol. 2 (Elsevier Science, Amsterdam, 1996), p. 642.
- [2] M. Doi and S. F. Edwards, *The Theory of Polymer Dynamics*, International Series of Monographs on Physics, Vol. 73 (Oxford University Press, Oxford, 2007), p. 391.
- [3] H. Löwen, *J. Phys. Condens. Matter* **13**, R415 (2001).
- [4] S. Fraden, G. Maret, D. L. D. Caspar, and R. B. Meyer, *Phys. Rev. Lett.* **63**, 2068 (1989).
- [5] H. Graf and H. Löwen, *Phys. Rev. E* **59**, 1932 (1999).
- [6] P. M. Johnson, C. M. v. Kats, and A. van Blaaderen, *Langmuir* **21**, 11510 (2005).
- [7] S. Roorda, T. van Dillen, A. Polman, C. Graf, A. van Blaaderen, and B. J. Kooi, *Adv. Mater.* **16**, 235 (2004).
- [8] A. M. Wierenga, T. A. J. Lenstra, and A. P. Philipse, *Colloids Surf. A* **134**, 359 (1998).
- [9] S. C. Glotzer and M. J. Solomon, *Nat. Mater.* **6**, 557 (2007).
- [10] V. N. Manoharan, M. T. Elsesser, and D. J. Pine, *Science* **301**, 483 (2003).
- [11] M. J. Solomon, R. Zeitoun, D. Ortiz, K. E. Sung, D. Deng, A. Shah, M. A. Burns, S. C. Glotzer, and J. M. Millunchick, *Macromol. Rapid Comm.* **31**, 196 (2009).
- [12] C. Quilliet, C. Zoldesi, C. Riera, A. van Blaaderen, and A. Imhof, *Eur. Phys. J. E* **27**, 13 (2008).

- [13] D. J. Kraft, W. S. Vlug, C. M. v. Kats, A. van Blaaderen, A. Imhof, and W. K. Kegel, *J. Am. Chem. Soc.* **131**, 1182 (2009).
- [14] T. C. Lubensky, *Science* **288**, 2146 (2000).
- [15] E. van den Pol, A. V. Petukhov, D. M. E. Thies-Weesie, D. V. Byelov, and G. J. Vroege, *Phys. Rev. Lett.* **103**, 258301 (2009).
- [16] A. Imperio, L. Reatto, and S. Zapperi, *Phys. Rev. E* **78**, 021402 (2008).
- [17] H. Löwen, *Phys. Rev. E* **50**, 1232 (1994).
- [18] M. C. Calderer, M. G. Forest, and Q. Wang, *J. Non-Newtonian Fluid Mech.* **120**, 69 (2004).
- [19] T. O. White, G. Ciccotti, and J.-P. Hansen, *Mol. Phys.* **99**, 2023 (2001).
- [20] J. Toner, Y. Tu, and S. Ramaswamy, *Ann. Phys.* **318**, 170 (2005).
- [21] E. Gauger and H. Stark, *Phys. Rev. E* **74**, 021907 (2006).
- [22] P. Dhar, T. M. Fischer, Y. Wang, T. E. Mallouk, W. F. Paxton, and A. Sen, *Nano Lett.* **6**, 66 (2006).
- [23] A. Walther and A. H. E. Müller, *Soft Matter* **4**, 663 (2008).
- [24] A. Erbe, M. Zientara, L. Baraban, C. Kreidler, and P. Leiderer, *J. Phys. Condens. Matter* **20**, 4215 (2008).
- [25] M. N. Popescu, S. Dietrich, and G. Oshanin, *J. Chem. Phys.* **130**, 194702 (2009).
- [26] G. Volpe, I. Buttinoni, D. Vogt, H. Kümmerer, and C. Bechinger, *Soft Matter* **7**, 8810 (2011).
- [27] S. van Teeffelen, U. Zimmermann, and H. Löwen, *Soft Matter* **5**, 4510 (2009).
- [28] R. Dreyfus, J. Baudry, M. L. Roper, M. Fermigier, H. A. Stone, and J. Bibette, *Nature (London)* **437**, 862 (2005).
- [29] H. C. Berg and L. Turner, *Biophys. J.* **58**, 919 (1990).
- [30] W. R. Diluzio, L. Turner, M. Mayer, P. Garstecki, D. B. Weibel, H. C. Berg, and G. M. Whitesides, *Nature (London)* **435**, 1271 (2005).
- [31] E. Lauga, W. Diluzio, G. Whitesides, and H. Stone, *Biophys. J.* **90**, 400 (2006).
- [32] J. Hill, O. Kalkanci, J. L. McMurry, and H. Koser, *Phys. Rev. Lett.* **98**, 068101 (2007).
- [33] V. B. Shenoy, D. T. Tambe, A. Prasad, and J. A. Theriot, *Proc. Natl. Acad. Sci. USA* **104**, 8229 (2007).
- [34] S. Schmidt, J. van der Gucht, P. M. Biesheuvel, R. Weinkamer, E. Helfer, and A. Fery, *Eur. Biophys. J.* **37**, 1361 (2008).
- [35] I. H. Riedel, K. Kruse, and J. Howard, *Science* **309**, 300 (2005).
- [36] D. M. Woolley, *Reproduction* **126**, 259 (2003).
- [37] B. M. Friedrich and F. Jülicher, *New J. Phys.* **10**, 123025 (2008).
- [38] T. L. Jahn and J. J. Votta, *Annu. Rev. Fluid Mech.* **4**, 93 (1972).
- [39] S. van Teeffelen and H. Löwen, *Phys. Rev. E* **78**, 020101 (2008).
- [40] B. ten Hagen, S. van Teeffelen, and H. Löwen, *Condens. Matter Phys.* **12**, 725 (2009).
- [41] B. ten Hagen, S. van Teeffelen, and H. Löwen, *J. Phys. Condens. Matter* **23**, 194119 (2011).
- [42] J. R. Howse, R. A. L. Jones, A. J. Ryan, T. Gough, R. Vafabakhsh, and R. Golestanian, *Phys. Rev. Lett.* **99**, 048102 (2007).
- [43] R. Vogel and H. Stark (private communication).
- [44] M. X. Fernandes and J. G. de la Torre, *Biophys. J.* **83**, 3039 (2002).
- [45] M. Makino and M. Doi, *J. Phys. Soc. Jpn.* **73**, 2739 (2004).
- [46] H. Brenner, *J. Colloid Sci.* **20**, 104 (1965).
- [47] H. Brenner, *J. Colloid Interface Sci.* **23**, 407 (1967).
- [48] H. N. Schulz and B. B. Jørgensen, *Annu. Rev. Microbiol.* **55**, 105 (2001).
- [49] K. N. Boyadzhiev, *College Math. J.* **30**, 23 (1999).
- [50] C. G. Gray and K. E. Gubbins, *Theory of Molecular Fluids: Fundamentals*, International Series of Monographs on Chemistry 9, Vol. 1 (Oxford University Press, Oxford, 1984), p. 626.
- [51] C. J. H. Schutte, *The Theory of Molecular Spectroscopy: The Quantum Mechanics and Group Theory of Vibrating and Rotating Molecules*, The Theory of Molecular Spectroscopy, Vol. 1 (North-Holland Publishing Company, Amsterdam, 1976), p. 512.
- [52] J. Happel and H. Brenner, *Low Reynolds Number Hydrodynamics: With Special Applications to Particulate Media*, 2nd ed., Mechanics of Fluids and Transport Processes, Vol. 1 (Kluwer Academic Publishers, Dordrecht, 1991), p. 553.
- [53] H. Risken, *The Fokker-Planck Equation: Methods of Solution and Applications*, 3rd ed., Springer Series in Synergetics, Vol. 18 (Springer, Berlin, 1996), p. 474.
- [54] A. W. C. Lau and T. C. Lubensky, *Phys. Rev. E* **76**, 011123 (2007).
- [55] U. Hassler, *Stochastische Integration und Zeitreihenmodellierung: Eine Einführung mit Anwendungen aus Finanzierung und Ökonometrie*, Statistik und ihre Anwendungen, Vol. 16 (Springer, Berlin, 2007), p. 325.
- [56] P. E. Kloeden and E. Platen, *Numerical Solution of Stochastic Differential Equations*, Applications of Mathematics: Stochastic Modelling and Applied Probability, Vol. 23 (Springer, Berlin, 2006), p. 636.
- [57] M. Abramowitz and I. A. Stegun, *Handbook of Mathematical Functions: With Formulas, Graphs, and Mathematical Tables*, 9th ed. (Dover Publications, New York, 1972), p. 1046.
- [58] W. H. Press, S. A. Teukolsky, W. T. Vetterling, and B. P. Flannery, *Numerical Recipes in C: The Art of Scientific Computing*, 2nd ed. (Cambridge University Press, Cambridge, 1992), p. 994.
- [59] G. B. Arfken and H. J. Weber, *Mathematical Methods for Physicists*, 6th ed. (Elsevier, Oxford, 2005), p. 1182.
- [60] J. C. Butcher, *Numerical Methods for Ordinary Differential Equations*, 2nd ed. (John Wiley & Sons, Chichester, 2008), p. 482.
- [61] H. H. Wensink and H. Löwen, *Phys. Rev. E* **78**, 031409 (2008).
- [62] R. Chelakkot, R. G. Winkler, and G. Gompper, *Europhys. Lett.* **91**, 14001 (2010).
- [63] J. Dunkel, V. B. Putz, I. M. Zaid, and J. M. Yeomans, *Soft Matter* **6**, 4268 (2010).
- [64] R. Wittkowski and H. Löwen, *Mol. Phys.* **109**, 2935 (2011).
- [65] M. Rex, H. H. Wensink, and H. Löwen, *Phys. Rev. E* **76**, 021403 (2007).
- [66] K. C. Leptos, J. S. Guasto, J. P. Gollub, A. I. Pesci, and R. E. Goldstein, *Phys. Rev. Lett.* **103**, 198103 (2009).
- [67] F. Peruani, A. Deutsch, and M. Bär, *Phys. Rev. E* **74**, 030904(R) (2006).
- [68] B. ten Hagen, R. Wittkowski, and H. Löwen, *Phys. Rev. E* **84**, 031105 (2011).
- [69] S. Rafai, L. Jibuti, and P. Peyla, *Phys. Rev. Lett.* **104**, 098102 (2010).
- [70] M. Hoffmann, C. S. Wagner, L. Harnau, and A. Wittemann, *Nano* **3**, 3326 (2009).
- [71] G. L. Hunter, K. V. Edmond, M. T. Elsesser, and E. R. Weeks, *Optics Express* **19**, 17189 (2011).